Transport of K^+ by Na^+-Ca^{2+},K^+ Exchanger in Isolated Rods of Lizard Retina

Giorgio Rispoli, Anacleto Navangione, and Vittorio Vellani
INFM, Dipartimento di Biologia dell'Università, Sezione di Fisiologia Generale, Via Borsari 46, 44100 Ferrara, Italy

ABSTRACT Transport of K^+ by the photoreceptor Na^+-Ca^{2+},K^+ exchanger was investigated in isolated rod outer segments (OS) by recording membrane current under whole-cell voltage-clamp conditions. Known amounts of K^+ were imported in the OS through the Ca^{2+}-activated K^+ channels while perfusing with high extracellular concentration of K^+, $[K^+]_o$. These channels were detected in the recordings from the OS, which probably retained a small portion of the rest of the cell. The activation of forward exchange (Na^+ imported per Ca^{2+} and K^+ extruded) by intracellular K^+, K_i^+, was described by first-order kinetics with a Michaelis constant, $K^{app}(K_i^+)$, of about 2 mM and a maximal current, I_{max}, of about −60 pA. $[Na^+]_i$ larger than 100 mM had little effect on $K^{app}(K_i^+)$ and I_{max}, indicating that Na_i^+ did not compete with K_i^+ for exchange sites under physiological conditions, and that Na^+ release at the exchanger intracellular side was not a rate-limiting step for the exchange process. Exchanger stoichiometry resulted in one K^+ ion extruded per one positive charge imported. Exchange current was detected only if Ca^{2+} and K^+ were present on the same membrane side, and Na^+ was simultaneously present on the opposite side. Nonelectrogenic modes of ion exchange were tested taking advantage of the hindered diffusion found for Ca_i^{2+} and K_i^+. Experiments were carried out so that the occurrence of a putative nonelectrogenic ion exchange, supposedly induced by the preapplication of certain extracellular ion(s), would have resulted in the transient presence of both Ca_i^{2+} and K_i^+. The lack of electrogenic forward exchange in a subsequent switch to high Na_o^+, excluded the presence of previous nonelectrogenic transport.

INTRODUCTION

Intracellular Ca^{2+} controls a variety of biochemical events that are involved in key physiological processes in every cell system, such as signal transduction, electrical excitability, excitation-contraction coupling, excitation-secretion coupling, cell growth, and cell-to-cell communication (Rasmussen and Rasmussen, 1990). The Na^+-Ca^{2+} exchanger is one of several cell mechanisms controlling Ca_i^{2+}, and its peculiarity lies in the ability to translocate Ca^{2+} into or out of the cytoplasm, depending upon the electrochemical gradient of the ions that provide the free energy for the process (Khananshvili, 1990; Laüger, 1991; Reeves, 1992). The vertebrate photoreceptor exchanger (Yau and Nakatani, 1984; Hodgkin et al., 1987) plays an important role in phototransduction, because the sustained exchanger activity in light induces $[Ca^{2+}]_i$ fall, which in turn triggers several mechanisms taking part in dark state recovery and light adaptation of the photoreceptor (Torre et al., 1986; Rispoli et al., 1988; Hsu and Molday, 1993; Kawamura, 1993; Lagnado and Baylor, 1994).

It has been found that the exchanger imports four Na^+ ions for every Ca^{2+} and K^+ ion extruded (forward mode of exchange) (Cervetto et al., 1989; Schnetkamp et al., 1989), thereby accounting for one net positive charge imported per exchange cycle (Yau and Nakatani, 1984; McNaughton et al., 1986; Hodgkin et al., 1987). Several studies have focused on the ion dependence of the exchange current, and the characteristics of the binding sites for Ca_i^{2+}, Na_o^+, Ca_o^{2+}, and K_o^+ have been studied in detail (Hodgkin and Nunn, 1987; Lagnado et al., 1988; Perry and McNaughton, 1993). To our knowledge, it has not yet been studied, with experiments in situ, the exchanger affinity for K_i^+ and the possible competition between K^+ and other ions for exchanger-binding sites at the intracellular side. Also, it has not been demonstrated yet that K^+ is transported in the forward mode with a stoichiometry of one K^+ ion per exchange cycle when the exchanger is far from equilibrium; moreover, it is still controversial whether K^+ is transported also by electrogenic or nonelectrogenic modes of ion exchange that are different from the forward mode (Schnetkamp, 1989; Lagnado and McNaughton, 1991; Perry and McNaughton, 1993). All of the above points are examined in the present study by performing fast ionic substitutions on isolated rod outer segments (OS) detached from the rest of the retina while recording by whole-cell voltage-clamp. The peculiar architecture of the OS, in which the entire transduction machinery, the cGMP channels, and the exchanger are segregated, makes the patch clamp recording from OS a powerful technique to study photoreceptor physiology (Sather and Detwiler, 1987; Cervetto et al., 1989; Rispoli and Detwiler, 1990, 1991; Rispoli et al., 1993; Perry and McNaughton, 1993). Preliminary reports of this work have been presented in conference proceedings (Rispoli and Navangione, 1992, 1993; Rispoli et al., 1994) and in a Ph.D. thesis (Navangione, 1994).

Received for publication 21 September 1994 and in final form 9 February 1995.

Address reprint requests to Dr. Giorgio Rispoli, INFM-Dipartimento di Biologia dell'Università, Sezione di Fisiologia Generale, Via Borsari 46, 44100 Ferrara, Italy. Tel.: 39-532-291472/291462; Fax: 39-532-207143; E-mail: mk5feqe3@icineca.

0006-3495/95/07/74/10 $2.00

MATERIALS AND METHODS

Preparation

OS were mechanically isolated from rods of the nocturnal lizards *Gekko gecko* and *Hemidactylus turcicus* (Rettili srl, Varese, Italy). The methods are described in detail elsewhere (Rispoli et al., 1993). Eyes were removed from dark-adapted animals previously decapitated and pithed. No differences in rod morphology and electrical recordings were found between the above species. OS were viewed with an infrared-sensitive CCD camera (XC-77CE Sony, Japan, illumination wavelength >850 nm) coupled to a modified inverted microscope (IMT-2 Olympus, Japan) equipped with Hoffmann optics (Modulation Optics, Greenvale, NY). Dissection was always made in the dark using an infrared viewer (Find-R-Scope, FJW Optical Systems, Palatine, IL) so that the retina, keeping its dark adaptation, was easily peeled off the eyecup and retained large amounts of intact photoreceptors. All experiments were performed in room light or in the dark at room temperature ($T \approx 19$–$24°C$): the results were unaffected by light.

Solutions and recording procedure

Electrical recordings were carried out using the "whole-cell" configuration of the patch-recording technique. Pipettes were fabricated from 100 μl of Drummond glass capillaries in the conventional manner (Hamill et al., 1981) and fire-polished to a pipette resistance of 7–11 MΩ. Pipettes were filled with one of the "intracellular" solutions indicated in the text with the subscript "i". The 0 Ca^{2+} solutions were buffered with 2 mM EGTA; all solutions were buffered to pH 7.4 with HEPES and NaOH, KOH, or tetraethylammonium hydroxide (TEA-OH) depending upon whether the solution contained high Na^+, high K^+, or 0 Na^+ and 0 K^+, respectively. The composition of Ringer solution was: 160 mM Na^+, 3.3 mM K^+, 1 mM Ca^{2+}, 1.7 mM Mg^{2+}, 165 mM Cl^-, 1.7 mM SO_4^{2-}, 2.8 mM HEPES, and 10 mM dextrose. Isotonic solutions contained 166 mM of the monovalent cation indicated in the text and 2 mM EGTA; the osmolality of the solutions that contained nonisotonic concentrations of the cations transported by the exchanger was adjusted to the Ringer osmolality with Li^+ and checked with a microosmometer (13/13 DR Roebling, Berlin, Germany). Current was recorded with an Axopatch 1D amplifier (Axon Instruments, Burlingame, CA). Holding potential was 0 mV unless specified otherwise and was corrected for junction potential when appropriate. Seal resistance, R_s, measured before rupturing the membrane patch, ranged between 10 and 40 GΩ. Only experiments without any change in series resistance, R_a (which ranged between 20 to 60 MΩ and was compensated, together with whole-cell capacitance, in all experiments), were considered. Input resistance, R_{in}, in the absence of sustained Ca^{2+}-activated channel activity, ranged between 1 and 30 GΩ. R_s, R_a, and R_{in} were measured as described in the legend of Fig. 7. The chamber was made from Teflon sandwiched between two glass microscope coverslips: the bottom one was coated with chloro-tri-*n*-butyl-silane to prevent cell sticking (Rispoli et al., 1993). The external solution was changed rapidly (typically in less than 50 ms) by moving horizontally with a computer-controlled stepping motor a multibarreled perfusion pipette placed in front of the recorded OS (Fig. 1, *inset*). No changes in the recordings were found by moving the OS within the same perfusion stream, nor by increasing the flow speed to the point of bending the OS, nor by switching between two identical solutions. Perfusion solution was removed by a peristaltic pump (Minipuls 2 Gilson, Villiers le Bel, France) connected to a drawn-down syringe inserted into the chamber. All chemicals were purchased from Sigma Chemical Co. (St Louis, MO) except charybdotoxin (Alomone labs, Jerusalem, Israel) and Chloro-tri-*n*-butyl-silane (Aldrich Chemical, Milwaukee, WI).

Data analysis

Data filtered at half the sampling frequency, using an eight-pole Butterworth filter (VBF/8 Kemo, Beckenham, U.K.), were digitized in PCM format and recorded on VHS tapes with a modified videorecorder (A.R. Vetter, Rebersburg, PA), or were digitized on- or off-line by a TL-1 DMA interface (Axon Instruments) and stored on erasable magneto-optical disks (M2511A, Fujitsu, Japan). Data were played back directly onto a chart recorder (L6514B Linseis, Selb, Germany) or a laser printer (Laserjet IIIP, Hewlett Packard, San Diego, CA) or a plotter (7470A, Hewlett Packard) using a commercial plotting program (Sigmaplot, Jandel Scientific, San Rafael, CA). Data fittings and statistics were done using Mathcad (MathSoft, Cambridge, MA) and original routines written in C-language (Borland, Scotts Valley, CA), and plotted with Sigmaplot. Values in text and figures are given as means ± SEM.

RESULTS

$[K^+]_i$ control with the aid of the Ca^{2+}-activated K^+ channels

The relationship between exchange current amplitude and $[K^+]_i$ was determined by controlling $[K^+]_i$ with the aid of the Ca^{2+}-activated channels, which were occasionally detected in the recordings from OS (Rispoli et al., 1993). Voltage-activated K^+ channels were described also in enzymatically dissociated OS (Hestrin and Korenbrot, 1987); however, the only OS conductances found in intact photoreceptors are the cGMP-gated channel and the exchanger (Baylor and Lamb, 1982; Lagnado et al., 1988). This indicates that the OS used in the present work probably retained a small piece of the inner segment, where the Ca^{2+}-activated channels are confined (Bader et al., 1982; Barnes and Hille, 1989). Some features of these channels are illustrated in Figs. 1 and 2. An OS, perfused with isotonic Na_i^+, was initially switched alternatively between three different solutions: isotonic K_o^+, isotonic Li_o^+, and isotonic Na_o^+ (Fig. 1); the current recorded in all of these solutions was 0 (which was set in cell attached condition). Switching the OS to a solution containing 20 mM K_o^+ and 1 mM Ca_o^{2+} elicited a large outward current due to reversed exchange (Ca^{2+} and K^+ imported per Na^+ extruded). Exchange current rapidly declined after attaining a peak (of ≈148 pA) with kinetics consistent with first-order inhibition of reversed exchange by Ca^{2+} accumulated in the cytoplasm (Perry and McNaughton, 1993). The recording became progressively noisier as channel activity was stimulated by Ca_i^{2+} accumulation. At this point, the current was 0 only in isotonic Li_o^+: a steady inward current, ascribed to K^+ flowing through the Ca^{2+}-activated channels, was recorded in isotonic K_o^+; a transient inward current, ascribed to forward exchange activation, was recorded in isotonic Na_o^+, and it declined to 0 as the Ca_i^{2+} and K_i^+ accumulated during reversed exchange were extruded by forward exchange. Once the OS was depleted of Ca_i^{2+} (and/or K_i^+), the current recorded in isotonic K_o^+, isotonic Li_o^+, and isotonic Na_o^+ was again 0.

Single Ca^{2+}-activated channel activity was usually discernible upon depolarizing the OS perfused with 30 mM Ca_i^{2+} and 124 mM K_i^+: the unitary current event was outward (K^+ flowing out of the OS) for holding potentials larger than −30 mV, and its amplitude, as well as the probability and duration of channel opening, increased with depolarization (Fig. 2). The channels were also blocked by extracellular charybdotoxin (100 nM) or TEA (20 mM) but

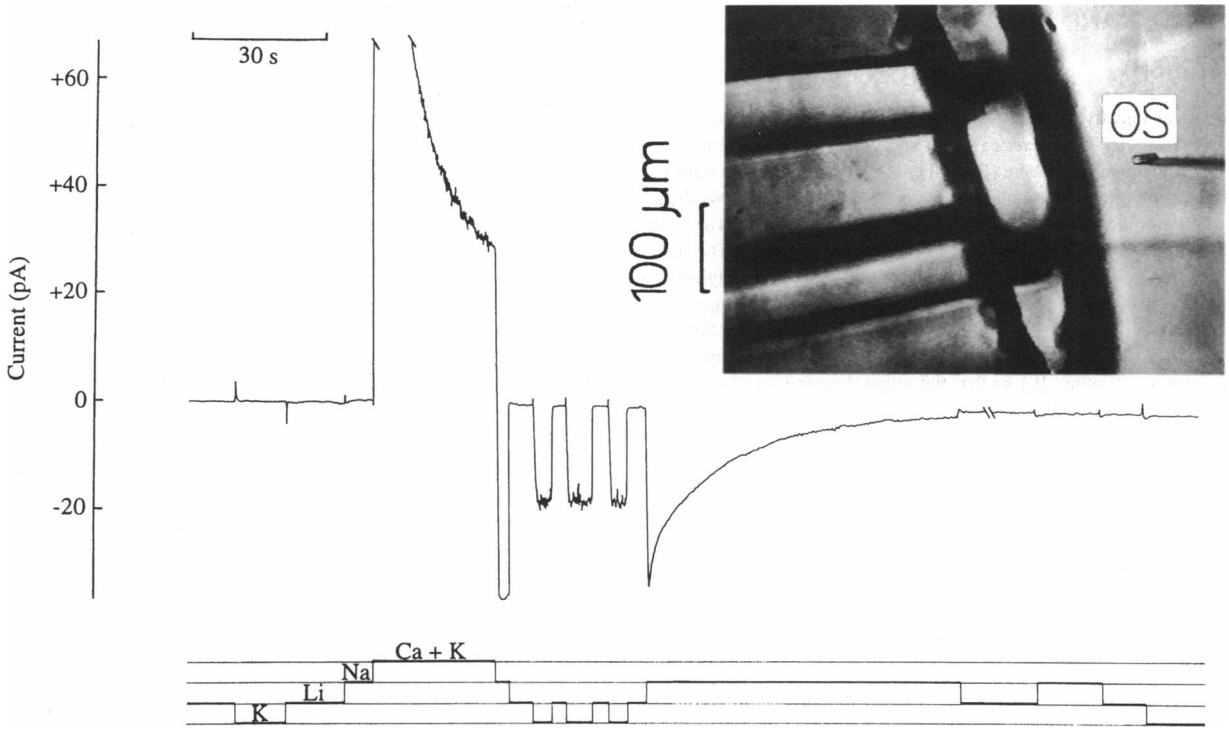

FIGURE 1 Turn on and turn off of Ca^{2+}-activated channels by controlling Ca_i^{2+} with the exchanger. Chart record of whole cell current from an OS perfused with isotonic Na_i^+. Isotonic K_o^+, isotonic Li_o^+ and isotonic Na_o^+ exposures before and after activating reversed exchange in 20 mM K_o^+ and 1 mM Ca_o^{2+}. Ca_i^{2+} and K_i^+ accumulated during reversed exchange elicited forward exchange in isotonic Na_o^+ and Ca^{2+}-activated channel activity in isotonic K_o^+. $R_s \approx 20$ GΩ, $R_a \approx 20$ MΩ, $R_{in} \approx 3$ GΩ. (*inset*) Single-frame video recording of an actual experiment. Solution change occurred once the OS crossed the boundary separating two adjacent streams, visible on the right.

not by Apamin (1 μM). All of these features are shared by the BK channels (Pallotta et al., 1981; reviewed by Garcia et al., 1991). Reversal of the unitary event upon hyperpolarization was only rarely observed due to the low probability of channel opening: sometimes reversed events were observed for voltages around −70 mV (Fig. 2), although the K^+ reversal potential, V_{rev}, was ≈−86 mV in these experiments (considering the activity coefficient for K_i^+ of about

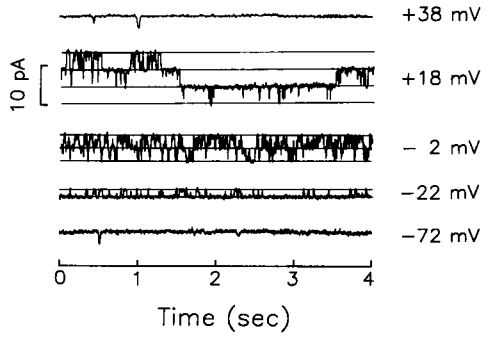

FIGURE 2 Current-voltage characteristics of the Ca^{2+}-activated channels. Single Ca^{2+}-activated channel activity (sampled at 2-ms intervals) after exchange and leak current subtraction in OS perfused with 124 mM K_i^+ and 30 mM Ca_i^{2+} and bathed in Ringer. Holding potential (corrected for junction potential) is shown near each trace. Up to three channels were activated upon depolarization ($R_s \approx 20$ GΩ, $R_a \approx 20$ MΩ, $R_{in} \approx 2$ GΩ); the trace at −72 mV is from a second OS ($R_s \approx 5$ GΩ, $R_a \approx 25$ MΩ, $R_{in} \approx 2$ GΩ).

0.8 and $T = 273$ K). This suggests that the "OS channels" are not as highly selective to K^+ as the BK channels, but they are also permeated by Na^+. However, no Ca^{2+}-activated channel activity was ever recorded by depolarizing an OS perfused with 30 mM Ca_i^{2+} and 124 mM Na_i^+, and bathed in 166 mM Li_o^+ or 166 mM Na_o^+ (8 OS), indicating that the "OS channels" are permeated by K^+ only (Hestrin and Korenbrot, 1987). On the other hand, in the present work it was found that K_i^+ diffusion was hindered (see next section and Discussion). The K^+ extrusion by forward exchange is then expected to reduce significantly $[K^+]$ at the intracellular side of the membrane with respect to the bulk $[K^+]_i$, giving a V_{rev} less negative than −86 mV. The conductance $g(V)$ of a K^+ channel is given by the voltage derivative of the Goldman-Hodgkin-Katz (GHK) equation:

$$g(V) = \frac{\partial i(V)}{\partial V} = \frac{\partial}{\partial V}$$

$$\left(\frac{P \cdot A \cdot V \cdot F^2 \cdot 10^3}{R \cdot T} \cdot \frac{[K^+]_i \cdot \exp\left(\frac{F \cdot V}{R \cdot T}\right) - [K^+]_o}{\exp\left(\frac{F \cdot V}{R \cdot T}\right) - 1} \right)$$

where $i(V)$ is the single-channel current at the membrane potential V, F is the Faraday's constant, R is the gas constant, P is the channel permeability, A is the area of the channel pore, and $[K^+]$ is in mol/l. The product $P{\cdot}A{\cdot}10^3$ was

calculated from the experimental $i(V)$ of Fig. 2 (for $V = -22, -2$ and $+18$ mV) using the GHK equation:

$$P \cdot A \cdot 10^3 = \frac{i(V)}{\frac{F^2 \cdot V}{R \cdot T} \cdot \frac{[K^+]_i \cdot \exp\left(\frac{F \cdot V}{R \cdot T}\right) - [K^+]_o}{\exp\left(\frac{F \cdot V}{R \cdot T}\right) - 1}}$$

It resulted that $g(V)$ was about the BK channel conductance (100 pS) if $[K^+]_i \approx 20$ mM (corresponding to $V_{rev} \approx -40$ mV). It can be estimated from $g(V)$ that the OS used in the present work contained, on average, no more than 7.0 ± 1.4 channels (range: 3–14 channels, 13 OS).

Depletion of endogenous K_i^+

To attain precise control over $[K^+]_i$, endogenous K_i^+ must first be depleted. Thus, the OS, perfused with millimolar $[Ca^{2+}]_i$ and $[Li^+]_i$, were initially bathed in Ringer so that any endogenous K_i^+ was extruded through forward exchange activation and washed out by the patch pipette. The time integral of this exchange current gave a lower limit for the number of endogenous K_i^+ ions at the beginning of whole-cell recording. The largest integral measured (in 24 experiments) corresponded to $[K^+]_i \approx 20$ mM (Fig. 3; the free OS volume, v, is estimated to be 1 pl: see Discussion), which was smaller than the physiological $[K^+]_i$ anyway (the smallest integral corresponded to $[K^+]_i \approx 2.6$ mM, and the average one to $[K^+]_i \approx 10.2 \pm 1.8$ mM, 8 OS). This discrepancy is expected, because the K_i^+ washout by the pipette and by the Ca^{2+}-activated channels cannot be ignored, given the large K^+ gradients between cytoplasm and extracellular space (pipette and bath) and the extended integration times (min) computed. It is also conceivable that some endogenous K_i^+ was lost during OS isolation (which was carried out in Ringer) and by exchanger activity before the whole-cell recording, stimulated by Ringer Na_o^+ and endogenous K_i^+ and Ca_i^{2+} (Ca_o^{2+} might also have entered the cytoplasm during OS isolation).

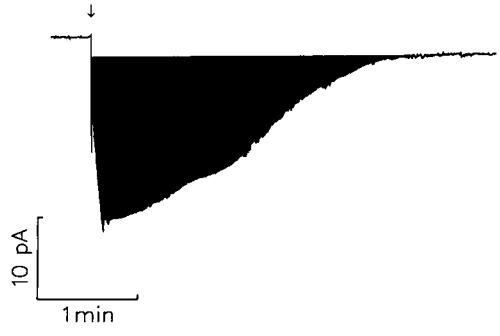

FIGURE 3 Endogenous K_i^+ washout upon bathing the OS in Ringer. Chart record of membrane breakthrough (occurred at the *arrow*) and whole-cell current from an OS perfused with 5–30 mM Ca_i^{2+} and 159–124 mM Li_i^+ or Na_i^+. The time integral of the exchange current elicited by endogenous K_i^+ in the OS shown (perfused with 30 mM Ca_i^{2+} and 124 mM Li_i^+) corresponded to the extrusion of ≈20 mM K_i^+. This experiment was carried out in bright light, so that ionic fluxes through the cGMP channels opened by possible endogenous nucleotides were eliminated through light activation of phosphodiesterase. $R_s \sim 25$ GΩ, $R_a \sim 30$ MΩ, $R_{in} \sim 2.5$ GΩ.

$K^{app}(K_i^+)$ estimate and hindered diffusion of intracellular ions

In the OS where the Ca^{2+}-activated channels were present, the relationship between exchange current amplitude and $[K^+]_i$ was estimated with the following protocol (Fig. 4). Once depleted of endogenous K_i^+, the 0 current level was checked by switching the OS to Isotonic Li_o^+, an ion that does not operate the exchanger (Hodgkin et al., 1987) and does not permeate either the Ca^{2+}-activated or the BK channels (Blatz and Magleby, 1987). A subsequent switch to isotonic K_o^+ loaded the OS with the K^+ flowing through the Ca^{2+}-activated channels and the leak (Fig. 4). Finally, a switch to isotonic Na_o^+ elicited a transient inward current, due to forward exchange activated by the pipette Ca^{2+} and by the K^+ imported during isotonic K_o^+ perfusion. The current declined to a small steady level (which was larger in OS with smaller R_{in}), representing essentially the inward leak driven by the junction potential between isotonic Na_o^+ and isotonic Li_o^+ (−3 mV). The time integral of the exchange current recorded in isotonic Na_o^+ (leak-subtracted) was equal to the time integral of the K^+ current in isotonic K_o^+ (the ratio between the two integrals was 1.0 ± 0.1, data from 10 measurements in 6 OS). This is consistent with an exchange stoichiometry of one K^+ ion extruded per charge imported, according to previous estimates (Cervetto et al., 1989). Furthermore, according to this stoichiometry, all of the K^+ imported through the Ca^{2+}-activated channels was

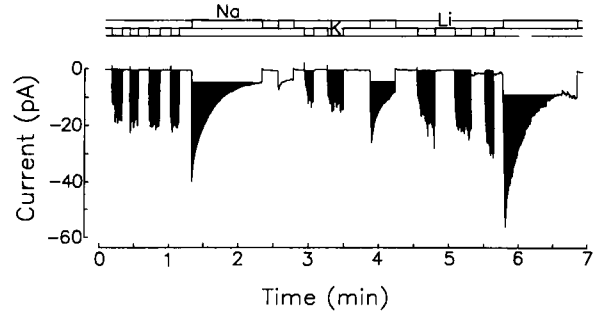

FIGURE 4 K^+ load through the Ca^{2+}-activated channels and K^+ extrusion through forward exchange. Chart record of whole-cell current from an OS (retaining Ca^{2+}-activated channels) perfused with 5 mM Ca_i^{2+} and 159 mM Li_i^+ and exposed to isotonic K_o^+, isotonic Li_o^+ or isotonic Na_o^+. All current in isotonic K_o^+ was carried by K^+ through the Ca^{2+}-activated channels and the leak. Current in isotonic Na_o^+ was basically the sum of exchange current (being activated by perfusion Na_o^+, pipette Ca_i^{2+} and K_i^+ imported during the previous exposure to isotonic K_o^+) and leak current. The three loads were, from left to right: $1.6 \cdot 10^9$, $6.2 \cdot 10^8$, $2.1 \cdot 10^9$ K^+ ions imported, respectively. The three exchange current integrals in isotonic Na_o^+ corresponded to: $1.5 \cdot 10^9$, $6.3 \cdot 10^8$, $2.2 \cdot 10^9$ charges imported, respectively. $R_s \sim 20$ GΩ, $R_a \sim 50$ MΩ, R_{in} varied from 1 to 0.7 GΩ from the beginning to the end of the recording.

extruded by the exchanger; thus, the K^+ washout by the patch pipette and the channels within the period of isotonic Na_o^+ perfusion was negligible. The time integral of the exchange current was not reduced appreciably by an intermediate switch to isotonic Li_o^+ for several tens of seconds between the isotonic K_o^+ and isotonic Na_o^+ perfusion (or up to a minute for access resistances >40 MΩ), showing that K^+ diffusion, indeed, was hindered. Thus, the time integral of the exchange current or the time integral of the K^+ current gave a reasonable measure of the actual number of K^+ ions trapped in the cytoplasm. However, the former time integral was smaller than the latter one for K^+ loads much larger than the measured $K^{app}(K_i^+)$ (see next section), because the K_i^+ washout became significant for large K^+ gradients between cytoplasm and extracellular space and for long integration times. Let I_K be the exchanger current peak measured in isotonic Na_o^+ (switching from isotonic Li_o^+), which is elicited by a K^+ load of size $[K^+]_i$. The plot of I_K vs. $[K^+]_i$ was described by first-order kinetics:

$$I_K = I_{max} \cdot \frac{[K^+]_i}{K^{app}(K_i^+) + [K^+]_i} \quad (1)$$

where $K^{app}(K_i^+)$ was ≈2 mM (assuming $v \approx 1$ pl) and I_{max} ≈ −60 pA (Fig. 5 *A*). I_{max} and $K^{app}(K_i^+)$ were in good agreement with the current peak amplitudes measured in isotonic Na_o^+ from OS in which K_i^+ was controlled directly with the patch pipette. These OS were kept in isotonic Li_o^+ for at least 2 min before switching to isotonic Na_o^+, to allow the $[K^+]$ at the level of the plasma membrane to equilibrate with the pipette $[K^+]$ by diffusion (the peak amplitude did not change if the Li_o^+ perfusion was kept for more than 10 min). The average peak, measured (in the absence of Ca^{2+}-activated channel activity) from OS perfused with extremely high $[Ca^{2+}]_i$ and $[K^+]_i$ (30 mM Ca_i^{2+} and 124 mM K_i^+), was −57 ± 3 pA (9 OS), whereas in OS perfused with 30 mM Ca_i^{2+} and 5 mM K_i^+ was −38 ± 5 pA (4 OS; Fig. 6 *b*). As expected, after the initial peak, the exchange current of Fig. 6 *b* declined to a steady level (of amplitude −12 ± 2 pA), because under these conditions the K^+ electrochemical gradient between the pipette and the intracellular side of the membrane was not enough to drive a sustained K^+ flux matching the peak rate of K^+ extrusion. A large exchange current decline was also recorded upon switching an OS perfused with 1 mM Ca_i^{2+} and 165 mM K_i^+ from isotonic Li_o^+ to isotonic Na_o^+ (Fig. 6 *a*; steady level: −6 ± 2 pA, 5 OS), showing that Ca_i^{2+} diffusion was also hindered. The $[K^+]_i$ near the plasma membrane, thus, is expected to fall below $K^{app}(K_i^+)$ as the exchange current declines in Fig. 6 *b*, whereas $[Ca^{2+}]_i$ is expected to fall below $K^{app}(Ca_i^{2+})$ as the exchange current declines in Fig. 6 *a*. It could be argued that Na^+ entering the OS accumulates in the cytoplasm, as K^+ does in the experiment of Fig. 4. Thus, the fall of exchange current in Fig. 6 *b* could also be ascribed to a competition between Na^+ and K^+ at the exchanger binding site for K_i^+, whereas the fall in Fig. 6 *a* to a competition between Na^+ and Ca^{2+} at the

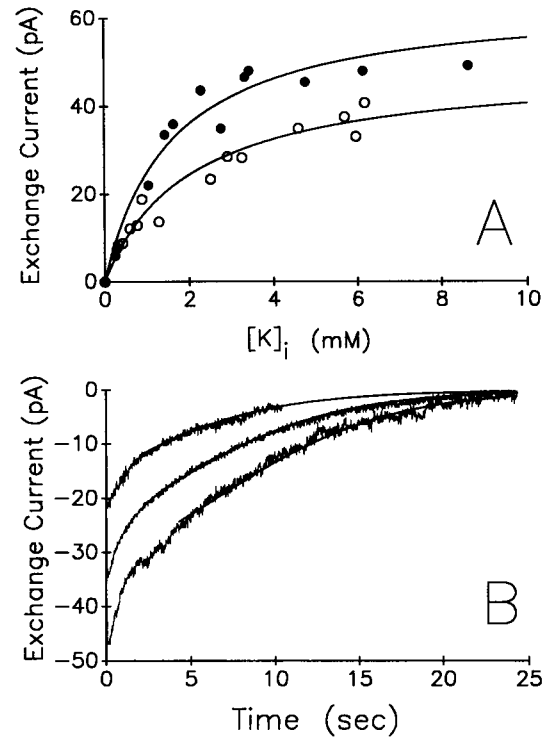

FIGURE 5 Theoretical fittings to the plot of I_{max} vs. $[K^+]_i$ and to the exchange current decline during extrusion of fixed K^+ loads. (*A*) Absolute value of exchange current peak measured in isotonic Na_o^+ vs. $[K^+]_i$. (●) Data from 16 measurements in 8 OS perfused with 5–30 mM Ca_i^{2+} and 159–124 mM Li_i^+; (○) data from 15 measurements in 5 OS perfused with 5–30 mM Ca_i^{2+} and 159–124 mM Na_i^+. Curves are first-order kinetics fittings (Eq. 1) to the data points, with $K^{app}(K_i^+)$ = 1.6 ± 0.4 mM and I_{max} = −64 ± 5 pA (●) and $K^{app}(K_i^+)$ = 2.0 ± 0.4 mM and I_{max} = −50 ± 4 pA (○). (*B*) Fittings to the exchange current decays of Fig. 4 (sampled at 10-ms intervals) with the numerical solution of the integral Eq. 2 with I_{max} = −64 pA and $K^{app}(K_i^+)$ = 3.3 mM. Fittings started after 2.0, 3.8, and 4.2 s from the beginning of the upper, middle, and lower trace, where exchange current amplitudes were 11.7, 17.2 and 23.9 pA, respectively.

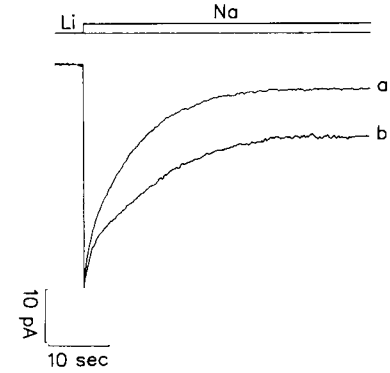

FIGURE 6 Hindered diffusion of Ca^{2+} and K^+. Chart record of exchange current peak followed by a large decay recorded in isotonic Na_o^+. (*a*) 1 mM Ca_i^{2+} and 165 mM K_i^+, $R_s \approx 10$ GΩ, $R_a \approx 30$ MΩ, $R_{in} \approx 1$ GΩ; (*b*) 30 mM Ca_i^{2+} and 5 mM K_i^+; $R_s \approx 15$ GΩ, $R_a \approx 40$ MΩ, $R_{in} \approx 2$ GΩ.

Ca_i^{2+}-binding site. However, the waveform in Fig. 6 *b* was affected little upon substituting Na_i^+ for Li_i^+ (119 mM) in the solution containing 5 mM K_i^+ and 30 mM Ca_i^{2+} (the

current peak upon switching from isotonic Li_o^+ to isotonic Na_o^+ was -34 ± 4 pA, 4 OS). Furthermore, both K^{app} (K_i^+) and I_{max} were affected little upon substituting Li_i^+ (124–159 mM) with Na_i^+ in the 5–30 mM Ca_i^{2+} solutions of the experiment of Fig. 4 (Fig. 5 *A*). It is then concluded that exchange current decline in Fig. 6 *b* was caused basically by the hindered diffusion of K_i^+.

Electrogenic and nonelectrogenic modes of ion transport

The data presented so far have been discussed assuming that K^+ transport occurs exclusively through a single electrogenic mode of ion exchange, in which Na^+ is imported and Ca^{2+} and K^+ are extruded. Other modes of ion exchange were suggested (Schnetkamp, 1989), but they were not confirmed by other groups (Lagnado and McNaughton, 1991; Perry and McNaughton, 1993). We detected electrogenic ion transport only if Ca^{2+} and K^+ were present on the same side of the membrane and Na^+ was simultaneously present on the opposite side (Rispoli and Navangione, 1993). This conclusion is based on a series of experiments where several combinations of intracellular (pipette ion(s): first column of Table 1) and extracellular solutions (preapplied or external ion(s): second column of Table 1) satisfying this requirement were tested. For instance, the electrogenic stoichiometries mCa^{2+}-nK^+ and nNa^+-lK^+ (n, m, and l are positive integers, $n \neq 2m$; exchange mode excluded, electrogenic: first and second line, fourth column of Table 1) were tested in the experiment of Fig. 7 where an OS perfused with isotonic K_i^+ was switched to 30 mM Ca_o^{2+} + 124 mM Li_o^+ and to isotonic Na_o^+. No current was detected in both solutions (once it was subtracted, the 1 pA-current given by the -3 mV junction potential between the Ca_o^{2+} + Li_o^+ and the Na_o^+). Similarly, no current was detected in any of the experiments listed in Table 1 (fourth column): it was then concluded that all of these putative electrogenic transport do not occur, or they do occur by generating a current smaller than the smallest current I_r detectable above the noise. In the latter case, an upper bound for the the ratio R_e between the turnover rate that would have been detectable and the maximal turnover rate τ_{max} (that generates the exchange current I_{max}) is given by:

$$R_e \leq \frac{I_r \cdot e}{q \cdot I_{max}}$$

where q is the charge transported per cycle by the putative electrogenic mode and e is the elementary charge. Because I_r is, at the most, 0.5 pA, it results $R_e \leq 7 \cdot 10^{-3}$ for $q = e$, corresponding to a turnover rate 140-fold smaller than τ_{max}. Such a low turnover is not expected to have any physiological relevance; thus, all of the putative electrogenic mode/s different than the Na^+-Ca^{2+},K^+ one were excluded.

The experiments so far discussed do not exclude that K^+ might also be transported through a putative nonelectrogenic mode of ion exchange. This possibility was tested taking advantage of the hindered diffusion of Ca^{2+} and K^+. Let us assume, for instance, that the exchanger might work with the stoichiometry $2mK^+$-mCa^{2+}. Then, an OS perfused with K_i^+ (pipette ion(s): first line, first column of Table 1) should accumulate Ca_i^{2+} upon perfusing it with Ca_o^{2+} (preapplied or external ion(s): first line, second column of Table 1; Fig. 7): a subsequent switch to isotonic Na_o^+ should then elicit a forward exchange current of amplitude I_n. Because no such current was detected, the stoichiometry under test does not occur or it does occur at a transport rate τ_n so that $I_n \leq I_r$. In the latter case, an upper bound for the ratio $R_{Ca} = \tau_n/\tau_{max}$ can be calculated as follows. Let us assume that, after perfusing with Ca_o^{2+} for a time $t_0 \approx 1$ min, the putative nonelectrogenic mode of exchange resulted in a Ca^{2+} load of size $[Ca^{2+}]_{iT}$. Then, after switching to isotonic $[Na^+]_o$, a current peak of amplitude I_{Ca} should be recorded, given by:

$$I_{Ca} = I_{max} \cdot \frac{[Ca^{2+}]_i}{K^{app}(Ca_i^{2+}) + [Ca^{2+}]_i}$$

where $K^{app}(Ca_i^{2+}) \approx 1.6$ μM and $[Ca^{2+}]_i$ is the free Ca^{2+} concentration in the presence of 2 mM EGTA (which was added to the isotonic K^+ solution; thus, the effect of the OS intracellular buffers can be neglected; Lagnado et al., 1992). Because $I_{Ca} \leq I_r$, then $[Ca^{2+}]_i \leq 15$ nM and $[Ca^{2+}]_{iT} \leq 0.5$ mM (the latter value is calculated from the apparent dissociation constant of EGTA). An upper bound for R_{Ca} is then:

$$R_{Ca} \leq \frac{[Ca^{2+}]_{iT} \cdot N_a \cdot v \cdot e}{t_0 \cdot I_{max}} - \frac{I_{leak}}{2 \cdot I_{max}}$$

where I_{leak} is the inward current carried by Ca^{2+} through the leak and N_a is the Avogadro's number. It results $R_{Ca} \leq 0.03$ if $I_{leak} = 0$ and $R_{Ca} \leq 0.02$ if $I_{leak} = 1$ pA (i.e., if all of the current recorded during Ca_o^{2+} perfusion is I_{leak}), giving a τ_n 40- to 50-fold smaller than τ_{max}. This upper bound for R_{Ca} can be

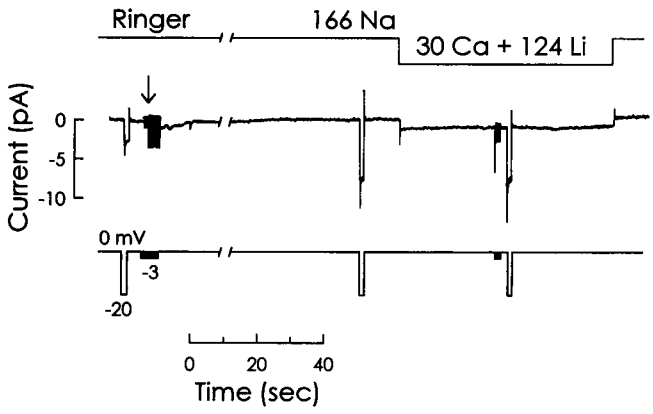

FIGURE 7 Test of electrogenic and nonelectrogenic modes of exchange. Chart record of whole-cell current recorded from an OS perfused with isotonic K_i^+. Breakthrough from cell attached to whole-cell occurred at the arrow. The peak amplitude of the current transient elicited by the -3 mV pulses (delivered at 10 Hz) was used to measure R_a, whereas the current amplitude elicited by the -20 mV pulse in cell attached and during whole-cell recording was used to measure R_s and R_{in}, respectively. $R_s \approx 8$ GΩ, $R_a \approx 40$ MΩ, $R_{in} \approx 3$ GΩ.

TABLE 1 Electrogenic and nonelectrogenic modes of ion exchange tested

Pipette ion(s) (mM)	Preapplied or external ion(s) (mM)	Exchange mode excluded	
		Nonelectrogenic	Electrogenic
166 K^+	30 Ca^{2+}	mCa^{2+}-$2mK^+$	mCa^{2+}-nK^{+} * mNa^+-nK^{+} ‡
166 K^+	124 K^+ + 30 Ca^{2+}	mCa^{2+}, nK^+-$(2m+n)K^+$ mCa^{2+}-$2mK^+$	nCa^{2+}, lK^+-mK^{+} § mCa^{2+}-nK^{+} *
30 Ca^{2+}	166 K^+	$2mK^+$-mCa^{2+}	nK^+-mCa^{2+} * nNa^+-mCa^{2+} *
83 Na^+ + 83 K^+	30 Ca^{2+}	$(n+l)Ca^+$-$2nNa^+$, $2lK^+$ mCa^{2+}-$2mNa^+$ mCa^{2+}-$2mK^+$	mCa^{2+}-nNa^+, lK^{+} ** mCa^{2+}-nNa^{+} * mCa^{2+}-nK^{+} * mNa^+-nK^{+} ‡ mNa^+-nK^+ , lNa^{+} ¶
124 Na^+ + 30 Ca^{2+}	166 K^+	$(2m+n)K^+$-mCa^{2+}, nNa^+ mK^+-mNa^+ $2mK^+$-mCa^{2+}	mK^+-nCa^{2+}, lNa^{+} § mK^+-nNa^{+} ‡ nK^+-mCa^{2+} * mNa^+-nCa^{2+}, lNa^{+} § nNa^+-mCa^{2+} *
124 K^+ + 30 Ca^{2+}	166 K^+		mK^+-lK^+, nCa^{2+} § nK^+-mCa^{2+} *
124 K^+ + 30 Ca^{2+}	30 Ca^{2+}		mCa^{2+}-nK^+, lCa^{2+} † mCa^{2+}-nK^{+} *
83 Na^+ + 83 K^+	166 K^+		mK^+-nNa^{+} ‡ mK^+-nK^+, lNa^{+} ¶
124 Na^+ + 30 Ca^{2+}	30 Ca^{2+}		mCa^{2+}-nNa^+, lCa^{2+} † mCa^{2+}-nNa^{+} *

Intracellular (pipette ion(s)) and extracellular (preapplied ion(s) or external ion(s)) ion combinations that gave no exchange current before and after Na_o^+ perfusion. The ions were preapplied for at least 1 min; each electrogenic or nonelectrogenic mode was tested in at least 2 OS. The notation nA-mB, lC (n, m, and l are positive integers) indicates that it is excluded the putative exchange of n ions A imported per m ions B and l ions C exported.

*$n \neq 2m$.

‡$m \neq n$.

§$m \neq 2n + l$.

**$2m \neq n + l$.

¶$m \neq n + l$.

†$2m \neq n + 2l$.

The OS in the experiments of the last four rows were not switched to Isotonic Na_o^+, because Ca^{2+} and K^+ were both perfused intracellularly or they were not applied to both sides of the membrane. The experiments requiring the perfusion with high Ca_i^{2+} were considered only if the Ca^{2+}-activated channels were not present in the recordings or if they were blocked by incorporating 20 mM TEA in all extracellular solutions.

applied to all of the nonelectrogenic modes that import Ca^{2+} listed in Table 1 (third column, lines 1, 2, 3, 5, 6, and 7). Analogously, an upper bound for the ratio R_K between $1/\tau_{max}$ and all of the turnover rates that would have been detectable in the case of nonelectrogenic import of K^+ (listed in Table 1, third column, lines 4, 8, 9, 10) is given by (using Eq. 1):

$$R_K \leq \frac{K^{app}(K_i^+) \cdot I_r \cdot N_a \cdot \nu \cdot e}{(I_{max} - I_r) \cdot t_0 \cdot I_{max}}$$

It resulted $R_K \leq 4{\cdot}10^{-4}$. The turnover numbers relative to R_{Ca} and R_K, if they exist, are so small in respect to τ_{max} that they are not expected to have a physiological relevance: it is then concluded that all of the nonelectrogenic modes listed in the third column of Table 1 do not occur.

DISCUSSION

The experiments described in this paper show that the photoreceptor exchanger extrudes K_i^+ via a site that binds K_i^+ with first-order kinetics with a Michaelis constant in the low millimolar range. This sets a lower limit for exchange stoichiometry of $n \geq 1$ K^+ ions extruded per exchange cycle (or charge imported) (Hodgkin et al., 1987; Yau and Nakatani, 1984). Because the number of charges imported during exchange activity in Na_o^+ after a K^+ load was equal to the number of K^+ ions loaded, then the only possibility is $n = 1$. Furthermore, no other modes of K^+ transport were found, either electrogenic or electrically silent: more generally, the only mode of ion exchange found was electrogenic and consisted of Na^+ imported per Ca^{2+} and K^+

extruded or vice versa. Finally, Ca_i^{2+} was not required for reverse exchange activation (Fig. 1), whereas it is necessary for reversed Na^+-Ca^{2+} exchange in other tissues, such as squid axon, squid optic nerve, barnacle muscle cells, guinea pig ventricular myocytes, and sarcolemma vesicles (reviewed by Dipolo and Beaugé, 1991).

Hindered diffusion of intracellular ions

The test of nonelectrogenic modes of ion exchange and the measure of $K^{app}(K_i^+)$ were both carried out taking advantage of the hindered diffusion of Ca_i^{2+} and K_i^+. It was found that, even for a relatively free diffusible ion such as K^+, it takes tens of seconds before a K^+ load is significantly washed out by the patch pipette. Poor diffusion between patch pipette and the cytoplasm was found experimentally (Push and Neher, 1988) and predicted theoretically, showing that the pipette tip is a significant barrier to diffusion in whole-cell configuration (Oliva et al., 1988). After the mathematical framework of Oliva et al. (1988), the time taken for K^+ to equilibrate with the patch pipette can be described in first approximation by a single exponential whose time constant is given by:

$$\tau = \frac{R_a \cdot v}{D \cdot \rho}$$

if K^+ is not buffered intracellularly nor transported through the plasma membrane, and where: $D = 1.96 \cdot 10^{-5}$ cm^2 s^{-1} is the diffusion coefficient for K^+, P = 100 Ω · cm is the resistivity of the pipette solution, v = 1 pl. τ ranged between 10 and 31 s for R_a = 20–60 MΩ. However, because the above calculation was carried out considering the OS as an "empty bag," it is expected that the actual diffusion of K^+ is even slower, as indeed was found in the present work, because the disk stack is a major cytoplasmic barrier opposing free solute diffusion (Olson and Pugh, 1993). In fact, it can be estimated that an OS 40 μm long and 8 μm in diameter can accommodate at least 1300 disks 0.015-μm thick, equally spaced at intervals of ~0.015 μm (Lamb et al., 1981), giving a free cytoplasmic volume of ~1 pl at the most. Olson and Pugh found that it takes more than 3 min for cGMP to diffuse from one end of the OS to the other. K^+ diffusion is probably faster than that, because it is not expected that K^+ is buffered as strongly as cGMP within the cytoplasm. However, the K^+ load occurs presumably at one end of the OS (that is, where a channel belonging to the inner segment should be located); thus, K_i^+ might not distribute uniformly along the OS within the time frame of the experiment of Fig. 4. The current peak recorded upon switching the loaded OS to isotonic Na_o^+ might then result from exchangers that are not all working at the same rate. However, K^+ loads larger than $K^{app}(K_i^+)$ (Fig. 5) gave exchange current peaks near I_{max} (which was determined independently: see discussion of Fig. 6), showing that within the loading time the $[K^+]_i$ attained a reasonably uniform saturating level along the OS. K^+ diffusion might occur preferentially along the pathway delimited by the plasma membrane and the disk stack.

Exchange current decline during extrusion of fixed K^+ loads

On the basis of the results so far discussed, the exchange current decays in isotonic Na_o^+ elicited by the three different K^+ loads of Fig. 4 can be predicted theoretically as follows. Let $I(t)$ be the exchange current at a certain time t, recorded from a cell of volume v, after a load of N_0 K^+ ions at time t = 0. Let N_m be the number of K^+ ions, determined experimentally, that gives a current amplitude of $I_{max}/2$ and from which $K^{app}(K_i^+)$ was calculated, according to the following equation:

$$K^{app}(K_i^+) = \frac{N_m \cdot m}{v}$$

where m is the atomic mass unit in g. If the exchanger is the only route for K^+ extrusion, and the relationship between $I(t)$ and the number of K^+ ions $N(t)$ is given by first-order kinetics for every t, then the current amplitude $I(t)$ in isotonic Na_o^+ of Fig. 4 can be computed numerically by solving iteratively the integral Eq. 2:

$$I(t) = I_{max} \cdot \frac{N_0 - (e^{-1}) \cdot \int_0^t |I(s)| \cdot ds}{N_m + N_0 - (e^{-1}) \cdot \int_0^t |I(s)| \cdot ds} \quad (2)$$

The computed solution, calculated with $K^{app}(K_i^+)$ and I_{max} close to the experimental values, fitted most of the exchange current decline, but not its very beginning, which fell faster than the theoretical curve, especially for large currents (Fig. 6 *B*). However, the relationship between $I(t)$ and $N(t)$, described by Eq. 2, may not hold for every t. In fact, ion extrusion rate during the abrupt exchange activation in Na_o^+ was probably not compensated immediately by ion diffusion rate from the cell interior, resulting in a transient fall in K^+ and/or Ca^{2+} at the level of the exchanger intracellular side. This, in turn, reduced the ion extrusion rate by the exchanger and increased the ion diffusion rate from the cell interior: the two rates eventually matched, and from this time on Eq. 2 then fits the experimental recordings. The kinetics of the very beginning of the current decline (time constant of about 2 s) is consistent with a radial diffusion some 50-fold faster than the longitudinal one (Lamb et al., 1981).

Influence of Na_i^+ on forward ion exchange

I_{max} and $K^{app}(K_i^+)$ were affected little by Na_i^+ concentrations up to 160 mM in the presence of saturating $[Ca^{2+}]_i$, showing that Na_i^+ does not compete with K_i^+ for exchange sites under physiological conditions. This is quite different with respect to the reversed exchange, where $K^{app}(K_o^+)$ rises when $[Na^+]_o$ is increased in the presence of saturating $[Ca^{2+}]_o$ (see Fig. 12 of Perry and McNaughton, 1993), suggesting that the exchange process is asymmetrical. Consistent with this view, the current peaks of reversed exchange recorded under saturating conditions (Fig. 1 protocol) were at least twice as large as those recorded in the forward mode (in the presence of 124 mM K_i^+, 30 mM Ca_i^{2+}, and 166 mM Na_o^+, Fig. 6 protocol). The insensitivity of forward exchange to Na_i^+ (in the presence of saturating $[Ca^{2+}]_i$) indicates that Na^+ release at the intracellular side is not a rate-limiting step in the exchange process, suggesting that $K^{app}(Na_i^+)$ has the same order of magnitude as $K^{app}(Na_o^+)$ (i.e., 93 mM; Lagnado et al., 1988). In conclusion, Na^+ unbinding from exchange sites can be regarded as diffusion-limited under physiological conditions. The $K^{app}(K_i^+)$ resulted about two orders of magnitude smaller than the physiological $[K^+]_i$ (which is larger than 100 mM: Somlyo and Waltz, 1985). Such a low value of $K^{app}(K_i^+)$ may have an important physiological meaning, according to the following reasoning. K^+ is pumped into the cell at the level of the inner segment (where the Na^+-K^+ ATPase pumps are segregated); thus, it is expected that K^+ does not readily reach the OS, especially its distal part. The K^+ extrusion by the exchanger may then cause a local depletion of $[K^+]_i$, which in turn may inhibit the exchanger itself if the $K^{app}(K_i^+)$ has the same order of magnitude of the physiological $[K^+]_i$. This inhibition would reduce the Ca^{2+} extrusion rate, and the resulting accumulation of Ca_i^{2+} would affect dramatically the photoreceptor light response. The low value of $K^{app}(K_i^+)$ makes, instead, a possible local depletion of $[K^+]_i$ ineffective in pumping efficiency: K_i^+ binding, therefore, is not expected to be a rate-limiting step for exchange activation under physiological conditions.

We are indebted to professors Luigi Cervetto, Vincent Torre, and Thomas W. Moon for helpful discussions and for reading the manuscript. Our thanks also to the anonymous reviewers for particularly helpful comments and suggestions. Many thanks to Messrs. Giuseppe Dia, Delia Fusetti, Andrea Margutti, Antonio Passarelli, and Guerrino Zampoli for invaluable technical assistance.

This work was supported by grants from Consiglio Nazionale delle Ricerche, the Ministero dell'Università e della Ricerca Scientifica e Tecnologica, and Human Frontiers Science Program.

REFERENCES

Bader, C. R., D. Bertrand, and E. A. Schwartz. 1982. Voltage-activated and calcium-activated currents studied in solitary rod inner segments from salamander retina. *J. Physiol.* 331:253–284.

Barnes, S., and B. Hille. 1989. Ionic channels of the inner segment of tiger salamander cone photoreceptors. *J. Gen. Physiol.* 94:719–743.

Blatz, A. L., and K. L. Magleby. 1987. Calcium-activated potassium channels. *Trends Neurosci.* 10:463–467.

Baylor, D. A., and T. D. Lamb. 1982. Local effects of bleaching in retinal rods of the toad. *J. Physiol.* 328:49–71.

Cervetto, L., L. Lagnado, R. J. Perry, D. W. Robinson, and P. A. McNaughton. 1989. Extrusion of Calcium from rod outer segment is driven by both Sodium and Potassium gradients. *Nature.* 337:740–743.

DiPolo, R., and L. Beaugé. 1991. Regulation of Na-Ca exchange. *Ann. N. Y. Acad. Sci.* 639:100–111.

Garcia, M. L., A. Galvez, M. Garcia-Calvo, V. F. King, J. Vazquez, and G. J. Kaczorowski. 1991. Use of toxins to study potassium channels. *J. Bioenerg. Biomembr.* 23:615–646.

Hamill, O. P., A. Marty, E. Neher, B. Sakmann, and F. J. Sigworth. 1981. Improved patch-clamp techniques for high resolution current recording from cells and cell-free membrane patches. *Pflügers Arch.* 391:85–100.

Hestrin, S., and J. I. Korenbrot. 1987. Voltage-activated potassium channels in the plasma membrane of rod outer segments: a possible effect of enzymatic cell dissociation. *J. Neurosci.* 7:3072–3080.

Hodgkin, A. L., and B. J. Nunn. 1987. The effect of ions on sodium-calcium exchange in salamander rods. *J. Physiol.* 391:371–398.

Hodgkin, A. L., P. A. McNaughton, and B. J. Nunn. 1987. Measurement of sodium-calcium exchanger in salamander rods. *J. Physiol.* 391:347–370.

Hsu, Y.-T., and R. S. Molday. 1993. Modulation of the cGMP gated channel of rod photoreceptor by calmodulin. *Nature.* 361:76–79.

Kawamura, S. 1993. Rhodopsin phosphorylation as a mechanism of cyclic GMP phosphodiesterase regulation by S-modulin. *Nature.* 362: 855–857.

Khananshvili, D. 1990. Cation antiporters. *Curr. Opin. Cell Biol.* 2:731–734.

Lagnado, L., and D. A. Baylor. 1994. Calcium controls light-triggered formation of catalytically active rhodopsin. *Nature.* 367:273–277.

Lagnado, L., L. Cervetto, and P. A. McNaughton. 1988. Ion transport by the Na:Ca exchange in isolated rod outer segments. *Proc. Natl. Acad. Sci. USA.* 85:4548–4552.

Lagnado, L., L. Cervetto, and P. A. McNaughton. 1992. Calcium homeostasis in the outer segment of retinal rods from tiger salamander. *J. Physiol.* 455:111–142.

Lagnado, L., and P. A. McNaughton. 1991. Net charge transport during sodium-dependent calcium extrusion in isolated salamander rod outer segments. *J. Gen. Physiol.* 98:479–495.

Lamb, T. D., P. A. McNaughton, and K.-W Yau. 1981. Spatial spread of activation and background desensitization in toad rod outer segments. *J. Physiol.* 319:463–496.

Läuger, P. 1991. Electrogenic Ion Pumps. Sinauer & Associates, Sunderland, MA.

McNaughton, P. A., L. Cervetto, and B. J. Nunn. 1986. Measurements of intracellular free calcium concentration in salamander rods. *Nature.* 322:261–263.

Navangione, A. 1994. Lo scambiatore Na:Ca, K dei fotorecettori retinici di vertebrato. Ph.D. thesis. University of Ferrara, Ferrara, Italy.

Oliva, C., I. S. Cohen, and R. T. Mathias. 1988. Calculation of time constants for intracellular diffusion in whole cell patch clamp configuration. *Biophys. J.* 54:791–799.

Olson, A., and E. N. Pugh. 1993. Diffusion coefficient of cyclic GMP in salamander rod outer segments estimated with two fluorescent probes. *Biophys. J.* 65:1335–1352.

Pallotta, B. S., K. L. Magleby, and J. N. Barrett. 1981. Single channel recordings of Ca^{2+}-activated K^+ currents in rat muscle cell culture. *Nature.* 293:471–474.

Perry, R. J., and P. A. McNaughton. 1993. The mechanism of ion transport by the Na^+-Ca^{2+},K^+ exchange in rods isolated from the salamander retina. *J. Physiol.* 466:443–480.

Push, M., and E. Neher. 1988. Rates of diffusional exchange between small cells and a measuring patch pipette. *Pflügers Arch.* 411:204–211.

Rasmussen, H., and J. E. Rasmussen. 1990. Calcium as intracellular messenger: from simplicity to complexity. *Curr. Top. Cell Regul.* 31: 1–109.

Reeves, J. P. 1992. Molecular aspects of sodium-calcium exchange. *Arch. Biochem. Biophys.* 292:329–334.

Rispoli, G., and P. B. Detwiler. 1991. Voltage dependence of light-sensitive and Na:Ca exchange currents in detached lizard retinal rod outer segments. *Biophys. J.* 59:434*a*. (Abstr.)

Rispoli, G., A. T. Fineberg, and P. B. Detwiler. 1990. Null current measurements provide estimate of intracellular Ca in rod outer segments. *Biophys. J.* 57:368*a*. (Abstr.)

Rispoli, G., and A. Navangione. 1992. Functional properties of the Na/Ca:K exchanger in vertebrate rods in situ. *Pflügers Arch.* 421:R22.

Rispoli, G., and A. Navangione. 1993. Photoreceptor Na/Ca:K exchanger is described by a consecutive cycle. *Pflügers Arch.* 424:R35.

Rispoli, G., A. Navangione, and V. Vellani. 1994. Intracellular K binding site properties of photoreceptor Na-Ca,K exchanger. *Pflügers Arch.* 428:R13.

Rispoli, G., W. A. Sather, and P. B. Detwiler. 1988. Effect of triphosphate nucleosides on the response of detached outer segments to low external calcium. *Biophys. J.* 53:390*a*. (Abstr.)

Rispoli, G., W. A. Sather, and P. B. Detwiler. 1993. Visual transduction in dialyzed detached rod outer segments from lizard retina. *J. Physiol.* 465:513–537.

Sather, W. A., and P. B. Detwiler. 1987. Intracellular biochemical manipulation of phototransduction in detached rod outer segment. *Proc. Natl. Acad. Sci. USA.* 84:9290–9294.

Schnetkamp, P. P. M.. 1989. Na:Ca or Na:Ca, K exchange in rod photoreceptors. *Prog. Biophys. Mol. Biol.* 54:1–29.

Schnetkamp, P. P. M., D. K. Basu, and R. T. Szerencsei. 1989. Na-Ca exchange in bovine rod outer segments requires and transports K. *Am. J. Physiol.* 257:C153–C157.

Somlyo, A. P., and B. Waltz. 1985. Elemental distribution in Rana Pipiens retinal rods: quantitative electron probe analysis. *J. Physiol.* 358: 183–195.

Torre, V., H. R. Matthews, and T. D. Lamb. 1986. Role of calcium in regulating the cyclic GMP cascade of phototransduction in retinal rods. *Proc. Natl. Acad. Sci. USA.* 83:7109–7113.

Yau, K.-W., and K. Nakatani. 1984. Electrogenic Na-Ca exchange in retinal rod outer segments. *Nature.* 311:661–663.